Comparison of Transmission Line Methods for Surface Acoustic Wave Modeling

[1]William WILSON, [2]Gary ATKINSON
[1]NASA Langley Research Center, Hampton, VA, USA,
[2]Virginia Commonwealth University, Richmond, VA, USA,
Phone: +1 (804) 827-0185, Email: GMAtkins@vcu.edu

Abstract: Surface Acoustic Wave (SAW) technology is low cost, rugged, lightweight, extremely low power and can be used to develop passive wireless sensors. For these reasons, NASA is investigating the use of SAW technology for Integrated Vehicle Health Monitoring (IVHM) of aerospace structures. To facilitate rapid prototyping of passive SAW sensors for aerospace applications, SAW models have been developed.

This paper reports on the comparison of three methods of modeling SAWs. The three models are the Impulse Response Method (a first order model), and two second order matrix methods; the conventional matrix approach, and a modified matrix approach that is extended to include internal finger reflections. The second order models are based upon matrices that were originally developed for analyzing microwave circuits using transmission line theory. Results from the models are presented with measured data from devices.

Keywords: Surface Acoustic Wave, SAW, transmission line models, Impulse Response Method.

1. Introduction

First order models of SAW devices are based upon the Impulse Response[1, 2]. These models do not take into account second order effects such as internal reflections, frequency shifts, or allow for any physical arrangement other than equal electrode widths and spaces. For more accurate results, a matrix based approach was developed [3]. This approach has been further refined and modified to include internal finger reflections [4]. The reflections occur when the thickness of the metallization is sizeable enough to result in significant reflections. The extensions are based upon matrices that were

originally developed for analyzing microwave circuits using transmission line theory. The modifications are accomplished by breaking up the SAW device into zones, where the area under a metalized region is treated as one zone, and the area without metallization is treated as another zone. The impedance discontinuities that occur at the edges of the metal fingers enable the simulation of the internal reflections of the mechanical acoustic wave. The modifications also enable incorporation of the different velocities for each region, which produces a more accurate characterization of the frequency response of the device. The modifications also allow for unequal finger widths and spacing.

In this paper, the three modeling methods are briefly discussed, then a comparison of the three models with results from prototype devices are presented.

2. First Order Modeling using the Impulse Response Method

The Impulse Response method [1] was used as the baseline for modeling the SAW device. This method is valid only for transducers where at least one of the two Inter-Digitated Transducers (IDTs) has a constant aperture or finger overlap [3]. This first order model includes both the mechanical and electrical behavior of SAW devices. It calculates the frequency response, the loss of the system, the admittance, and parameters for circuit simulators. This model assumes constant and equal spacing and finger widths. A simple circuit model (Fig. 1) can be used to convey the basic elements of the Impulse Response Model. The figure shows the source voltage and both the source and load impedances which are not part of the model. In the circuit model C_T is the total capacitance, $B_a(f)$ is the acoustic susceptance and $G_a(f)$ is the radiation conductance.

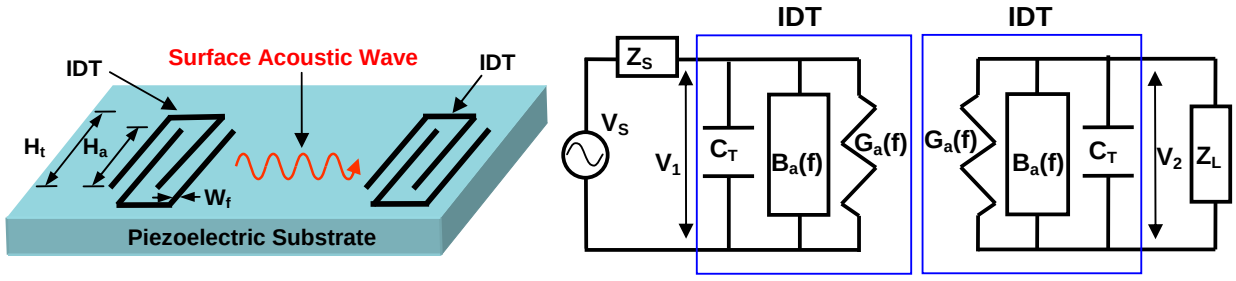

(a) (b)

Fig. 1. (a) Basic SAW delay line and (b) the circuit model used in the Impulse Response Modeling. C_T is the total capacitance, $B_a(f)$ is the acoustic susceptance, and $G_a(f)$ is the radiation conductance.

The frequency response of a SAW device can be calculated by using the Impulse Response Model and is given by [5]:

$$H(f) = 20\log\left(4k^2 C_s H_a f_0 Z_r N_p^2 \left(\frac{\sin(X)}{X}\right)^2 e^{-j\left(\frac{N_p+D}{f_0}\right)}\right). \quad (1)$$

Where k is the piezoelectric coupling coefficient, C_s is the capacitance per finger pair and unit length, H_a is the aperture or overlap height of the fingers, f_0 is the center or synchronous frequency, N_p is the number of finger pairs, f is the frequency, D is the delay length between the IDTs, and Z_r is the wave impendence and X is given by:

$$X = N_p \pi \frac{(f - f_0)}{f_0}. \quad (2)$$

3. Conventional Matrix Method

The matrices discussed in this work were originally developed for analyzing microwave circuits using transmission line theory. The methodology utilizing transmission matrices was modeled on the approach given by Campbell [3]. This method is based upon the Mason equivalent circuit using the crossed field technique (Fig. 1b) [4]. In this method, for modeling purposes, a SAW device is modeled as two IDTs with two electrical ports, and two acoustic ports. The acoustic ports represent mechanical waves traveling into and out of the IDT. The electrical ports represent the current and voltage of the IDT. The matrix for a SAW delay line is simply the multiplication of the matrices for the two IDTs and a matrix for the delay in between (Fig. 2).

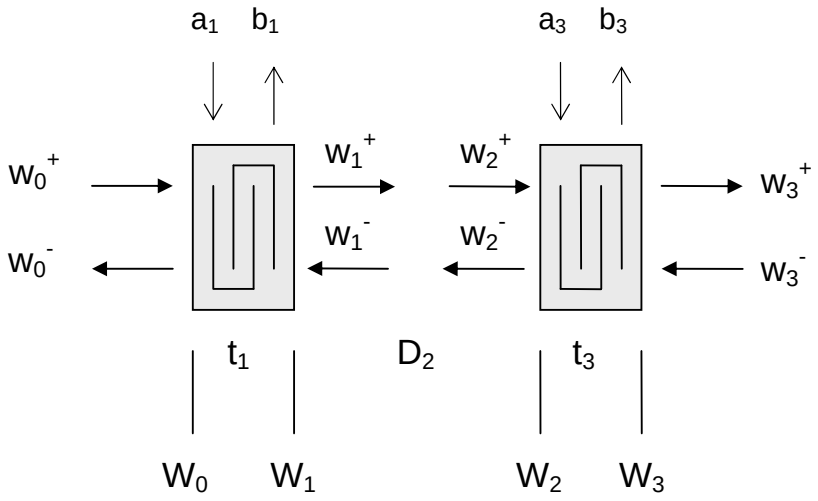

Fig. 2. Transmission line matrix model of a complete SAW delay line.

The transmission matrix is often used because it can be cascaded easily. The complete SAW device matrix is given by:

$$[SAW(f)] = [T_1(f) D_1(f) T_2(f)]. \tag{3}$$

Where f is the frequency, $T_i(f)$ is the transmission matrix for an IDT, and $D(f)$is the delay matrix. The delay matrix ($D(f)$) is modeled after an acoustic transmission line and is given by:

$$[D(f)] = \begin{bmatrix} e^{j\frac{2f\pi}{v}d} & 0 \\ 0 & e^{-j\frac{2f\pi}{v}d} \end{bmatrix}, \tag{4}$$

where λ is the wavelength at the center or synchronous frequency and d is the distance between the reference planes, or in this case the center of the two IDTs.

Each IDT is modeled separately as a single transmission matrix ($T_i(f)$) with one electrical port, and two acoustic ports (Fig. 3).

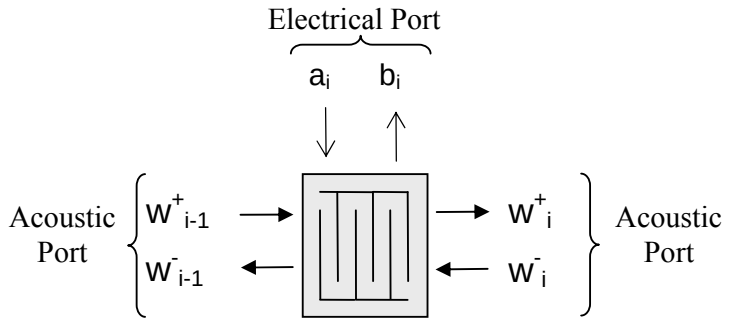

Fig. 3. Transmission matrix model of an IDT.

This allows the acoustic waves (W_i) and electrical parameters (a_i and b_i) to be related through the use of transmission matrix $T_i(f)$ in:

$$\begin{pmatrix} W_{i-1}^{+} \\ W_{i-1}^{-} \\ b_i \end{pmatrix} = T_i(f) \begin{pmatrix} W_i^{+} \\ W_i^{-} \\ a_i \end{pmatrix} . \tag{5}$$

The transmission matrix is decomposed into sub-elements, given by

$$T_i(f) = \begin{pmatrix} t_{11}(f) & t_{12}(f) & t_{13}(f) \\ -t_{12}(f) & t_{22}(f) & t_{23}(f) \\ st_{13}(f) & -st_{23}(f) & t_{33}(f) \end{pmatrix} . \tag{6}$$

The elements of the transmission matrix are given by:

$$t_0(f) = \frac{G_a(f)(R_s + Z_e)}{(1 + j\theta_e(f))} , \tag{7}$$

$$t_{11}(f) = (1 + t_0(f))e^{j\theta_t(f)} , \tag{8}$$

$$t_{12}(f) = t_0(f) , \tag{9}$$

$$t_{13}(f) = \frac{\sqrt{(2G_a(f)Z_e)}}{1 + j\theta_e(f)} e^{\frac{j\theta_t(f)}{2}} , \tag{10}$$

$$t_{22}(f) = (1 - t_0(f))e^{-j\theta_t(f)} , \tag{11}$$

$$t_{23}(f) = -t_{13}(f)e^{-j\theta_t(f)} , \tag{12}$$

$$t_{33}(f) = \frac{2j\theta_c(f)}{1 + j\theta_e(f)} . \tag{13}$$

The symmetry factor s is based upon the number of fingers (N_t):

$$s = -1^{N_t} \quad . \tag{14}$$

The transit angles θ_e , θ_c, and θ_t,are given by:

$$\theta_e(f) = (\omega C_t + B_a)(R_s + Z_e) \quad , \tag{15}$$

$$\theta_c(f) = \omega C_t (R_s + Z_e) \quad , \tag{16}$$

$$\theta_t(f) = N_t \frac{\lambda}{2} \delta \quad . \tag{17}$$

The combined load or source impedance is Z_e, and R_s is the combined IDT metal and lead resistance. The frequency detuning parameter (δ) is given by

$$\delta = \frac{2\pi(f - f_0)}{v} - k_{11} \quad , \tag{18}$$

where v is the velocity, and k_{11} is the mutual-coupling coefficient and is given by:

$$k_{11} = k_{11p} + k_{11m} \frac{h}{\lambda} + k_{11s} \left(\frac{h}{\lambda} \right)^2 \quad . \tag{19}$$

where h is the height of the metal fingers. The mutual coupling coefficient parameters k_{11p}, k_{11m}, and k_{11s}, are material dependent, for quartz they are 0.0004, 0.02, and 7.9 [3]. The total capacitance for the IDT is given by:

$$C_t = \frac{(N_t - 1)}{2} C_s \quad , \tag{20}$$

where C_s is the capacitance per unit length for a pair of fingers. The conductance (G_a) is given by [3]:

$$G_a = 8k^2 C_s f_0 (N_t - 1)^2 \left(\frac{\sin\left(\frac{\theta_t}{2}\right)}{\frac{\theta_t}{2}} \right)^2 \quad . \tag{21}$$

And finally, the susceptance (B_a) is given by [3]:

$$B_a = 16k^2 C_s f_0 (N_t - 1)^2 \left(\frac{\sin(\theta_t) - \theta_t}{\theta_t^2} \right) , \tag{22}$$

4. Modified Matrix Method

For more accurate results than are given by the first order approach or the conventional method, the matrix approach was extended to include second order effects such as the internal finger reflections [3, 6]. The model divides an IDT into ½ wavelength sections. These sections are further divided into zones. Two of the zones are un-metalized areas (1/8 of a wavelength) around one zone that is comprised of a metal finger (1/4 of a wavelength). Each zone is modeled by a transmission line matrix equivalent circuit (Fig. 4). Two identical circuits model the un-metalized areas, while the middle circuit models the area under the metal finger. The transmission matrix relates the SAW voltages V_1 and V_2, to the currents I_1 to I_2 respectively. The acoustic wave is assumed to have entered from the left and travels through the element towards the right. In this model Z_u and Z_m are the acoustic impedances for the metalized and un-metalized areas, C_0 is the capacitance for a single finger, θ_u and θ_m are the acoustic angles of the substrate, and the turns ratio of the transformer is assumed to be 1:1.

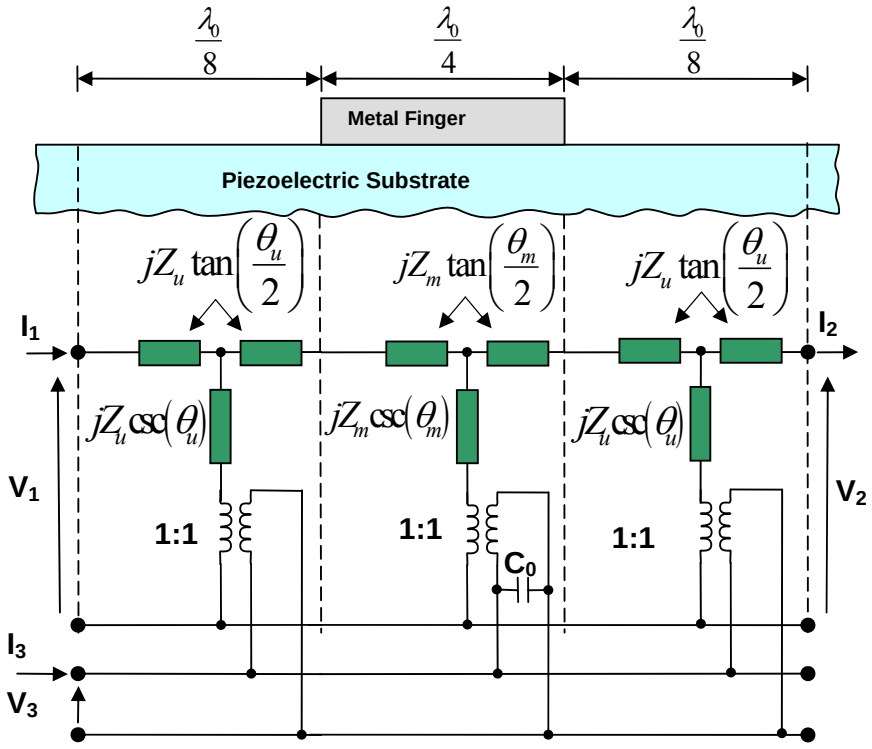

Fig. 4. Crossfield Model using Mason Equivalent Circuit for a ½ wavelength section of an IDT.

The transmission matrix representing the middle area shown in Fig. 4 is the circuit for a metalized region that is assumed to be lossless and is given by:

$$\left[R_m(f)\right] = \begin{bmatrix} \cosh(j\theta_m(f)) & Z_m \sinh(j\theta_m(f)) \\ \frac{1}{Z_m}\sinh(j\theta_m(f)) & \cosh(j\theta_m(f)) \end{bmatrix}. \tag{23}$$

The transmission matrix (23) is determined by the acoustic angle θ_m and the metalized region's impedance Z_m. The impedance Z_m is calculated with:

$$Z_m(f) = \frac{1}{k^2 C_s H_a f_m}, \tag{24}$$

where k^2 is the piezoelectric coefficient, C_s is the capacitance for a single pair of electrodes per unit length, and H_a is the aperture width. The acoustic angle of the substrate θ_m, is given by

$$\theta_m(f) = \frac{\pi}{2}\frac{f}{f_m} \ , \tag{25}$$

where f is the frequency, and f_m is the frequency shift caused by the velocity change as the acoustic wave travels under the metalized area:

$$f_m = \frac{v_m}{\lambda} \ . \tag{26}$$

Where v_m is the acoustic wave velocity under the metalized area and λ is the wavelength of the device. The metalized velocity (v_m) is 3134 m/s for ST cut Quartz.

The matrix (23) calculates the parameters for the metalized area, but cannot be used for the un-metalized sections. This leads to the transmission matrix ($R_u(f)$) for the un-metalized region as is given by:

$$\left[R_u(f)\right] = \begin{bmatrix} \cosh(j\theta_u(f)) & Z_u \sinh(j\theta_u(f)) \\ \frac{1}{Z_u}\sinh(j\theta_u(f)) & \cosh(j\theta_u(f)) \end{bmatrix} . \tag{27}$$

The transmission matrix (27) is determined by the acoustic angle θ_u and the un-metalized region's impedance Z_u. The impedance Z_u is calculated with:

$$Z_u(f) = \frac{1}{k^2 C_s H_a f_0} \ . \tag{28}$$

where f_0 is the synchronous frequency of the acoustic wave under for the un-metalized area. The acoustic angle of the substrate θ_u, is given by

$$\theta_u(f) = \frac{\pi}{4}\frac{f}{f_0} \ . \tag{29}$$

where f_0 is the synchronous frequency of the acoustic wave, which is calculated using the acoustic wave velocity under the un-metalized area. The un-metalized velocity (v) is 3158 m/s for ST cut Quartz.

To find the transmission matrix for the ½ wavelength periodic element ($R_T(f)$) one must multiply the three matrices together for both metalized region and the un-metalized regions adjacent to it:

$$\left[R_t(f)\right] = \left[R_u(f)\right]\left[R_m(f)\right]\left[R_u(f)\right] \ . \tag{30}$$

To find the transmission matrix ($Q(F)$) for an entire IDT one simply raises the ($R_T(f)$) matrix to the power of $2N_p$:

$$\left[IDT_1(f)\right] = \left[R_t(f)\right]^{2N_p} \ . \tag{31}$$

Where N_p is the number of electrode pairs, so $2N_p$ is the total number of electrodes in the IDT.

The matrix for a SAW delay line is simply the multiplication of the matrices for the two IDTs and the delay or space between the IDTs. The SAW matrix is given by:

$$\left[SAW(f)\right]=\left[IDT_1(f)\right]\left[D_1(f)\right]\left[IDT_2(f)\right] . \tag{32}$$

5. Prototype Design

A simple SAW delay line that consists of two identical un-apodized IDTs was chosen as a prototype to illustrate the capability of the models. Each IDT has 63 finger pairs that are 17 μm wide. The spacing between the fingers is 17 μm also. The center or synchronous frequency is 46.44 MHz, or a wavelength of 68 μm. The aperture height is 2730 μm. The delay length between the IDTs is 10 wavelengths or 680 μm. The design was fabricated on two different ST cut quartz wafers. One with a single side polished, and one wafer with both sides polished. The aluminum thickness is 50 nm for the wafer with a single side polished and 250 nm for the wafer with both sides polished. Also, a 112.78 MHz device was fabricated on the single side polish wafer. It has 90 pairs of 7 μm fingers, a wavelength of 28 μm, and an aperture height of 1105 μm. The delay length is 104 wavelengths or 2.904 mm.

6. Results

All three methods adequately model the frequency response and amplitude for the main lobe and the first two side lobes for cases without any mass loading due to the metal fingers (Fig. 5). The modified matrix more accurately captures the frequency shift due to the mass loading of the metal fingers. In Figure 6, the ideal first order model (impulse response model) and the conventional matrix results are both centered about the synchronous frequency. The measured results and the Modified matrix results are both shifted down in frequency due to velocity changes from mass loading effects.

When comparing the measured data from the two figures, it is noticeable that the main lobe peak of Fig. 5 does not have the same artifacts as are seen on the peak of the main lobe in Fig. 6. These artifacts are due in part from bulk waves that are reflected from the polished bottom surface of the wafer. The roughness of the non-polished surface disperses the bulk waves which results in diminished artifacts in the main lobe peak (Fig. 5). Also note that the peak in Fig 6 is shifted farther away by mass loading than the peak in Fig. 5.

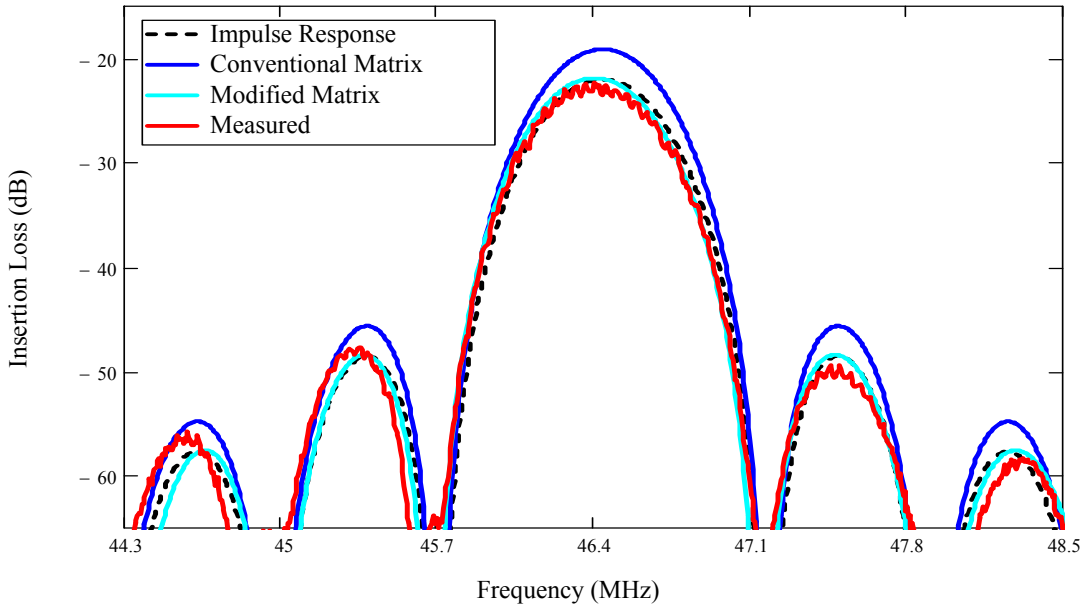

Fig. 5. Comparison of model results with data from a single side polish wafer, with 50 nm of aluminum.

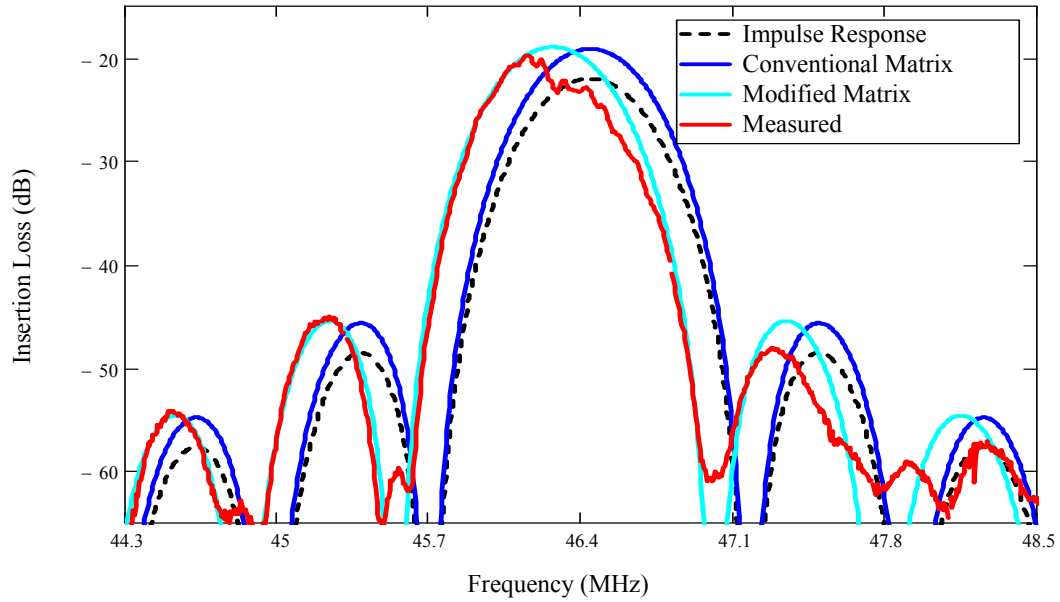

Fig. 6. Comparison of model results with data from a double side polish wafer, with 250 nm of aluminum.

While the models work well for the side lobes of low frequency devices at 46.4 MHz, as the frequency increases the accuracy goes down for the side lobes (Fig. 7). The measured data shows higher order effects and noise at 112.8 MHz that is not present in the lower frequency device data. These results show that opportunities exist for improvements to both the models and the test setup. The inclusion of higher order terms to the models will increase their fidelity. The fidelity of the test setup can be improved by dicing the wafer or by the inclusion of gating functions in the time domain. Time gating will allow the removal of unwanted reflections from adjacent devices on the test wafer without having to dice the wafer and add absorber material to the devices. Essentially the addition of the gating functions will allow us to take data on the wafer, while achieving the results as if the devices had been packaged in an ideal manner.

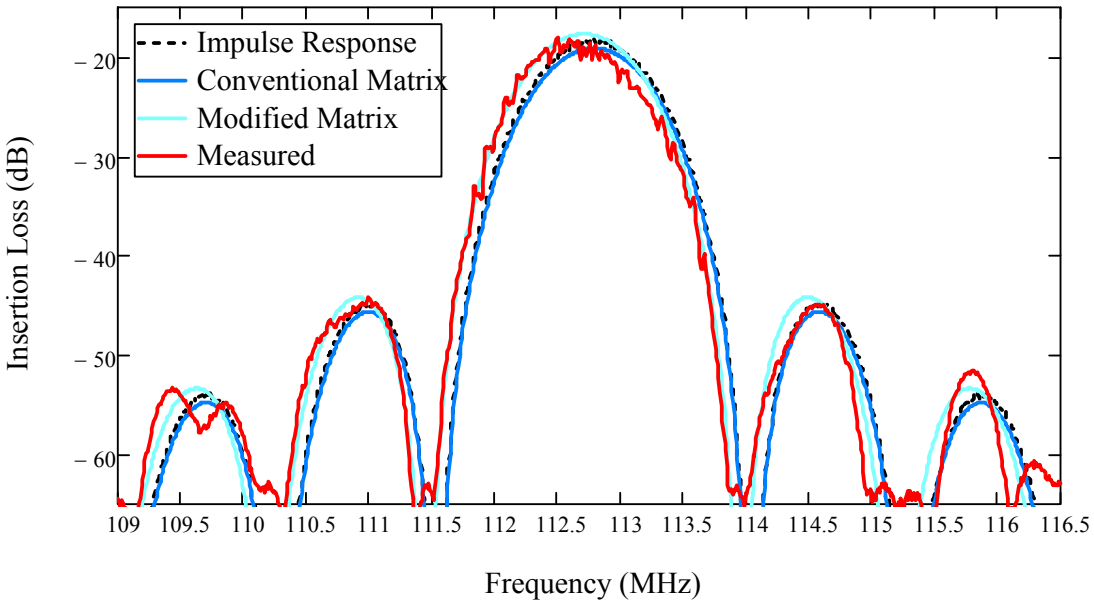

Fig. 7. Comparison of model results with data from a single side polish wafer, with 50 nm of aluminum.

7. Conclusion

In this paper, results from prototype devices are compared to the Impulse Response model, a conventional matrix model, and a modified matrix model. In the absence of mass loading from the metal fingers and the associated frequency shift, all three methods model the main lobe and next two side lobes fairly well. However, the results show that the modified matrix methods more accurately modeled second order effects such as frequency shift due to the metal thickness of the IDT fingers. Neither the Impulse response method nor the conventional matrix method model the frequency shift. Therefore, the modified matrix method is the most accurate for a wider range of parameters such as finger metal thickness. Future work will include a comparison the Coupling of Modes, the Impulse Response model, and the modified matrix model. Also, to achieve higher fidelity our future models will include higher order terms. To improve our wafer level test setup, time gating in the time domain will be added to remove artifacts that would not be present if the devices were packaged in an ideal manner with absorber materials.

References

[1]. C. S. Hartmann, Jr., D. T. Bell and R. C. Rosenfeld, "Impulse Model Design of Acoustic Surface-Wave Filters," *Microwave Theory and Techniques, IEEE Transactions on,* vol. 21, pp. 162-175, 1973.

[2]. W. C. Wilson and G. M. Atkinson, "Frequency Domain Modeling of SAW Devices for Aerospace Sensors," *Sensors & Transducers* vol. 2, pp. 42-50, October 8 2007.

[3]. C. Campbell, *Surface Acoustic Wave Devices for Mobile and Wireless Communications*, New York, NY, Academic Press, 1998.

[4]. W. P. Mason, *Physical acoustics* vol. 1A, New York and London, Academic Press, 1964.

[5]. V. M. Ristic, *Principles of acoustic devices*, New York, NY, Wiley, 1983.

[6]. H. Y. Tung, "The Design of Surface Acoustic Devices using the Transmission Matrix Method," I-Shou University, 2005.